Proceedings of the 7th International Symposium on Cavitation
CAV2009 – Paper No. ##
August 17-22, 2009, Ann Arbor, Michigan, USA

Cavity flow with surface tension past a flat plate

Yuriy Savchenko
Institute of Hydromechanics of the NAS
Kiev, Ukraine

Yuriy Semenov
Institute of Hydromechanics of the NAS
Kiev, Ukraine

ABSTRACT

The effect of surface tension forces on the cavity flow parameters is considered for steady flow past a rounded-edge plate perpendicular to the incident flow. The fluid is assumed to be ideal, weightless, and incompressible. The problem is solved in a parameter region by finding analytical expressions for the flow potential and the function that conformally maps the parameter region into the flow region in the physical plane. The dynamic boundary condition includes the surface tension force, which is proportional to the free boundary curvature, and allows one to obtain an integral equation in the velocity magnitude on the free boundary. The integral equation is solved numerically by the method of successive approximations. The results of calculations of the effect of the Weber number and the plate edge radius on the geometry of the cavity and the drag coefficient of the plate are presented.

INTRODUCTION

The surface tension force arises at the phase interface as a result of the work done by the reversible isothermokinetic process of free boundary formation. According to the Young–Laplace equation, a pressure jump proportional to the surface curvature develops across the phase interface. This complicates the dynamic boundary condition because the velocity on the cavity boundary depends on the cavity curvature. A significant difficulty in accounting for surface tension stems from the fact that, according to the theory of jets in ideal fluids, in the limiting case of the absence of surface tension the free surface curvature at the point of flow separation from a sharp edge becomes infinite. Introducing even a small surface tension coefficient into such a model results in an infinite force and the absence of cavitation.

Attempts to account for the surface tension force in cavity flow problems have been made in Refs. [1 – 4]. In Ref. [3], the case of small surface tension coefficients is considered using the method of matched asymptotic expansions. In this case, the free boundary curvature at the separation point is equal to the curvature of the plate. Such a formulation of the problem gives rise to waves on the free surface. As shown in Ref. [4], these waves are unfeasible because they would require energy supply from infinity. In Refs. [1 – 2] it is assumed that at the flow separation point the slope of the flow boundary is a discontinuous function. According to the theory of jets in ideal fluids, that assumption results in an infinite velocity and curvature at the separation point. This gives no way of obtaining a continuous transition to the limiting case of the absence of surface tension, for which the velocity at the separation point is finite.

In this work we show that the point of flow separation from a smooth surface in the presence of surface tension is determined by the Brillouin–Villat condition in exactly the same manner as for neglect of surface tension. A sharp edge is considered as the limiting case when the curvature of the rounded plate edge tends to infinity. In this formulation, no physical contradictions occur in the solution of the problem, and the flow with zero surface tension force results as a limiting case.

MATHEMATICAL FORMULATION AND THE METHOD OF SOLUTION

We consider symmetric flow of an ideal weightless fluid past a curved, in the general case, obstacle with the formation of a cavity downstream of the body. A schematic of the flow is shown in Figure 1. The wedge-shaped body of vertex angle α has a rectilinear part, which smoothly changes into a circular arc of radius R. The cavity detaches from the rounded part of the body at point O at angle β_0 and closes on the curvilinear contour CDB, on which the velocity distribution is specified. Point C, which is the inflection point on the contour OCB, corresponds to the end of the cavity and the start of the closing contour. The maximum width H of the body is chosen as a characteristic dimension.

On the cavity boundary, the surface tension force gives rise to a pressure jump, which is determined from the Young–Laplace equation

$$P - P_c = \tau\chi \qquad (1)$$

where P is the pressure on the fluid of the cavity boundary, P_c is the pressure in the cavity, τ is the surface tension coefficient, $\chi = d\gamma/ds$ is the cavity curvature, and γ is the slope of the cavity contour. In the neighborhood of the separation point O, the cavity curvature becomes negative because for the chosen direction of increasing coordinate s its value decreases when moving along the cavity contour. As follows from Eq. (1), surface tension reduces the pressure in the fluid on the cavity boundary.

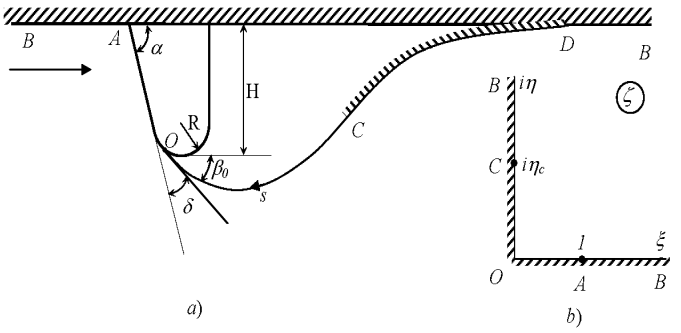

Figure 1: Schematic of cavity flow past curvilinear contour: *a*) physical plane; *b*) parameter region

The Bernoulli equation for the irrotational flow under consideration

$$\frac{V^2}{2} + \frac{P}{\rho} = \frac{V_\infty^2}{2} + \frac{P_\infty}{\rho} \tag{2}$$

gives the velocity on the cavity boundary, which, in view of Eq. (1), can be written in dimensionless form as follows

$$v = V \Big/ V_\infty = \sqrt{1 + \sigma - \frac{2\chi H}{We}} \tag{3}$$

where $We = \dfrac{\rho V_\infty^2 H}{\tau}$ is the Weber number and $\sigma = \dfrac{P - P_c}{\frac{1}{2}\rho V_\infty^2}$ is the cavitation number.

Since the flow is irrotational, we can introduce its potential ϕ and the stream function ψ, which is the harmonic conjugate of ϕ, both defined in a parameter region, for which the first quadrant is chosen (Figure1*b*). By the conformal mapping theorem, the images of three points can be fixed arbitrarily; let the points $\varsigma = 0$, $\varsigma = 1$, and $\varsigma = \infty$ in the parameter region correspond to points *O, A*, and *B* in the physical plane.

The mathematical formulation of the problem is as follows: find the complex flow potential $w = \phi + i\psi$ that meets the nonpassing condition on the body and the dynamic boundary condition (3) on the free boundary. Following Zhukovsky's [5] and Chaplygin's [6 – 7] methods, the problem is solved by constructing expressions for the complex velocity, dw/dz, and the derivative of the complex potential, $dw/d\varsigma$, in the region of the parametric variable ς. If these expressions are found, the correspondence between the parameter region and the physical flow region is given by the mapping function

$$z(\varsigma) = z_0 + \int_0^\varsigma \frac{dw/d\varsigma'}{dw/dz} d\varsigma' . \tag{4}$$

A method for the construction of expressions for the complex velocity and the derivative of the complex potential for a mixed boundary value problem is reported in Ref. [8]. One has to find the function dw/dz that satisfies the following boundary conditions

$$\begin{aligned} &\arg\left(\frac{dw}{dz}\right) = \begin{cases} -\beta(\xi), & 0 < \xi < 1, \quad \eta = 0, \\ 0, & 1 < \xi < \infty, \quad \eta = 0, \end{cases} \\ &\left|\frac{dw}{dz}\right| = v(\eta), \qquad\qquad 0 < \eta < \infty, \quad \xi = 0. \end{aligned} \tag{5}$$

Here, $\beta(\xi)$ is the slope in the physical plane as a function of the real-axis coordinate in the parameter region. This angle decreases when moving along the body from point O to point A, $\beta(1) = -\alpha$; $v(\eta)$ is the velocity magnitude on the free boundary as a function of the imaginary-axis coordinate in the parameter region.

An expression for the complex velocity that satisfies the above boundary conditions (5) has the form

$$\begin{aligned} \frac{dw}{dz} = v_0 \left(\frac{\varsigma - 1}{\varsigma + 1}\right)^{\alpha/\pi} \exp\left[\frac{1}{\pi}\int_0^1 \frac{d\beta}{d\xi'} \ln\left(\frac{\varsigma - \xi'}{\varsigma + \xi'}\right) d\xi' - \right. \\ \left. - \frac{i}{\pi}\int_0^\infty \frac{d \ln v}{d\eta'} \ln\left(\frac{i\eta' - \varsigma}{i\eta' + \varsigma}\right) d\eta' \right] \end{aligned} \tag{6}$$

When $\varsigma = \xi$ and $\varsigma = i\eta$ are substituted in turn into Eq. (6), it is apparent that the boundary conditions (5) for the complex velocity are satisfied.

The derivative of the complex potential is found by Chaplygin's singularity method [7]

$$\frac{dw}{d\varsigma} = K\varsigma \tag{7}$$

where K is a scale factor, which will be determined below. Substituting Eqs. (6) and (7) into Eq. (4) allows one to find the derivative of the mapping function $z = z(\varsigma)$ as well as the dependences $s = s(\xi)$ (the coordinate along the body contour) and $s = s(\eta)$ (the coordinate along the free boundary):

$$\frac{dz}{d\varsigma}=\frac{K\varsigma}{v_0}\left(\frac{\varsigma+1}{\varsigma-1}\right)^{\alpha/\pi}\exp\left[\frac{i}{\pi}\int_0^\infty\frac{d\ln v}{d\eta'}\ln\left(\frac{i\eta'-\varsigma}{i\eta'+\varsigma}\right)d\eta'-\frac{1}{\pi}\int_0^1\frac{d\beta}{d\xi'}\ln\left(\frac{\varsigma-\xi'}{\varsigma+\xi'}\right)d\xi'\right], \quad (8)$$

$$s(\eta)=-\int_0^\eta\left|\frac{dz}{d\varsigma}\right|_{\varsigma=i\eta}d\eta=-\int_0^\eta\frac{1}{v(\eta)}\left|\frac{dw}{d\varsigma}\right|_{\varsigma=i\eta}d\eta=-K\int_0^\eta\frac{\eta'}{v(\eta')}d\eta', \quad (9)$$

$$s(\xi)=\int_0^\xi\left|\frac{dz}{d\varsigma}\right|_{\varsigma=\xi'}d\xi'.$$

The scale factor K appearing in Eqs. (9) is determined from the condition for the length of the wetted part of the body

$$S_w=s(\xi)\big|_{\xi=1}. \quad (10)$$

Cavity closure scheme. The closure of the cavity is specified implicitly by specifying the velocity distribution along the closing contour *CDB*. The velocity on the contour *CD* decreases from the value $v_c=\sqrt{1+\sigma-2\chi H/We}$ at point *C* down to the value v_∞ at point *D*. The velocity distribution along the segment *CD* can be specified by the linear function

$$v^*(s')=v_c(1-s')+v_\infty s', \quad (11)$$

where $s'=(s-s_c)/S_{CD}$ and s_c is the coordinate of the cavity closure point *C* determined from the cavity closure condition, which has the form

$$\mathrm{Im}\left(\int_{\varsigma=\infty}\frac{dz}{d\varsigma}d\varsigma\right)=-\mathrm{Im}\left(\int_{\varsigma'=\infty}\frac{dz}{d\varsigma'}\frac{d\varsigma'}{\varsigma'^2}\right)=-\frac{i\pi}{4}\underset{\varsigma'=0}{res}\frac{d^2}{d\varsigma'^2}\left(\frac{dz}{d\varsigma'}\varsigma'\right)=0, \quad (12)$$

where $\varsigma'=1/\varsigma$.

Taking the integral in Eq. (12) along an infinitely large contour with the help of the residue theorem, we obtain the following equation

$$\int_0^1\frac{d\beta}{d\xi'}\xi'd\xi'+\int_0^\infty\frac{d\ln v}{d\eta'}\eta'd\eta'+\alpha=0. \quad (13)$$

The velocity distribution $v(\eta)=v^*[s(\eta)]$ along the cavity closure contour *CD* must satisfy Eq. (12). This is achieved with the help of the coordinate s_c in Eq. (11), which affects the velocity distribution along the free boundary.

Condition for cavity detachment from the rounded edge. The point of flow separation from the rounded edge is determined from the Brillouin–Villat condition [7], which is equivalent to the extremum condition for the velocity magnitude function on the contour of the body

$$\lim_{s\to0}\frac{d\ln v}{ds}=0. \quad (14)$$

Using the relation $\frac{d\ln v}{ds}=\frac{d\ln v/d\xi}{ds/d\xi}$, differentiating the function $v(\xi)=|dw/dz|_{\varsigma=\xi}$, and substituting the result into Eq. (14), we obtain the following equation

$$\int_0^1\frac{d\beta}{d\xi'}\frac{d\xi'}{\xi'}-\int_0^\infty\frac{d\ln v}{d\eta'}\frac{d\eta'}{\eta'}+\alpha=0. \quad (15)$$

Eq. (15) is an equation in the length S_w of the wetted part of the body because this quantity affects the function $\beta(\xi)=\beta[s(\xi)]$, $0<s<S_w$.

Boundary conditions and corresponding integro-differential equations.

For the known shape of the curved section of the body given by the function $\beta(s)$, the function $\beta(\xi)$ is determined by the numerical solution of the integro-differential equation

$$\frac{d\beta}{d\xi}=\frac{d\beta}{ds}\frac{ds}{d\xi} \quad (16)$$

or

$$\frac{d\beta}{d\xi}=\chi[s(\xi)]\frac{K\xi}{v_0}\left(\frac{1+\xi}{1-\xi}\right)^{\alpha/\pi}\exp\left[-\frac{1}{\pi}\int_0^1\frac{d\beta}{d\xi'}\ln\left(\frac{\xi'-\xi}{\xi'+\xi}\right)d\xi'-\frac{1}{\pi}\int_0^\infty\frac{d\ln v}{d\eta'}\left(\pi-2\tan^{-1}\left(\frac{\eta'}{\xi}\right)\right)d\eta'\right]$$

where $\chi(s)$ is the curvature of the body given as a function of the arc length s.

In order to derive an integral equation in the function $d(\ln v)/d\eta$, we first need to get an expression for the curvature χ along the cavity boundary, i.e. along the imaginary axis η of the parameter region. The slope of the free surface is determined from equation (6) as follows

$$\beta(\eta)=-\arg\left(\frac{dw}{dz}\right)=\frac{2\alpha}{\pi}\tan^{-1}\eta-\alpha-\frac{1}{\pi}\int_0^1\frac{d\beta}{d\xi'}\left(\pi-2\tan^{-1}\frac{\eta}{\xi'}\right)d\xi'+\frac{1}{\pi}\int_0^\infty\frac{d\ln v}{d\eta'}\ln\left|\frac{\eta'-\eta}{\eta'+\eta}\right|d\eta'$$

Differentiating the above equation and taking into account equation (9), we find the curvature of the free surface

$$\chi = \frac{d\gamma/d\eta}{ds/d\eta} = -\frac{2v}{\pi K\eta}\left(\frac{\alpha}{1+\eta^2} + \int_0^1 \frac{d\beta}{d\xi'}\frac{\xi' d\xi'}{\xi'^2+\eta^2} - \int_0^1 \frac{d\ln v}{d\eta'}\frac{\eta' d\eta'}{\eta'^2-\eta^2}\right) \quad (17)$$

By substituting equation (17) into the dynamic boundary condition (3), we obtain the following integral equation

$$\frac{2}{\pi}\int_0^\infty \frac{d\ln v}{d\eta'}\frac{\eta' d\eta'}{\eta'^2-\eta^2} = \frac{2\alpha/\pi}{1+\eta^2} + \frac{2}{\pi}\int_0^\infty \frac{d\beta}{d\xi'}\frac{\xi' d\xi'}{\xi'^2+\eta^2} + \frac{WeK\eta}{2Rv(\eta)}(1+\sigma-v^2) \quad (18)$$

where

$$v(\eta) = v_0 \exp\left(\int_0^\eta \frac{d\ln v}{d\eta'} d\eta'\right) \qquad \text{and} \qquad v_0 = \sqrt{1+\sigma+2/We}\,.$$

Curvature of the free surface at the point of separation. In order to evaluate the curvature of the free surface at the separation point, where at $\eta = 0$ equation (17) has an indeterminate form, we differentiate the numerator and denominator of equation (17) to obtain:

$$\chi_0 = \lim_{\eta\to 0}\chi(\eta) = \lim_{\eta\to 0}\left\{-\frac{1}{K}\frac{dv}{d\eta}\left(\frac{1}{1+\eta^2} + \frac{2}{\pi}\int_0^\infty \frac{d\beta}{d\xi'}\frac{\xi' d\xi'}{\xi'^2+\eta^2} - \frac{2}{\pi}\int_0^\infty \frac{d\ln v}{d\eta'}\frac{\eta' d\eta'}{\eta'^2-\eta^2}\right)\right\} + \lim_{\eta\to 0}\left\{\frac{2\eta v}{K}\left(\frac{1}{(1+\eta^2)^2} + \frac{2}{\pi}\int_0^\infty \frac{d\beta}{d\xi'}\frac{\xi' d\xi'}{(\xi'^2+\eta^2)^2} + \frac{2}{\pi}\int_0^\infty \frac{d\ln v}{d\eta'}\frac{\eta' d\eta'}{(\eta'^2-\eta^2)^2}\right)\right\} \quad (19)$$

The first limit in the above equation equals zero due to the flow separation condition (15). In order to evaluate the second term containing the singular integrals, we have to estimate the behavior of the functions $d\ln v/d\eta$ at $\eta \to 0$ and $d\beta/d\xi$ at $\xi \to 0$. From the Brillouin-Villat condition (14) it follows

$$\frac{d\ln v}{ds} = \frac{d\ln v}{d\eta}\Big/\frac{ds}{d\eta} = 0\,.$$

In view of equation (9), it can be seen that for $\eta \to 0$ $ds/d\eta = K\eta/v(\eta) \sim \eta$. Therefore, from equation (14) it follows

$$\lim_{\eta\to 0}\frac{d\ln v}{d\eta}\frac{1}{\eta} = 0\,, \quad \Rightarrow \quad \frac{d\ln v}{d\eta} \sim \eta^{1+\alpha}\,, \quad \eta \to 0\,, \quad \alpha \ge 0\,. \quad (19)$$

The behavior of the function $d\beta/d\xi$ is determined in a similar way

$$\frac{d\beta}{d\xi} = \frac{d\beta}{ds}\frac{ds}{d\xi} = \chi(\xi)\frac{ds}{d\xi} = \chi(\xi)\frac{K\xi}{v(\xi)}\,, \;\Rightarrow\; \frac{d\beta}{d\xi} \sim \chi_0^*\frac{K}{v_0}\xi\,, \quad (21)$$

where $v_0 = \lim_{\xi\to 0} v(\xi) = \lim_{\xi\to 0}\left|dw/dz\right|_{\varsigma=\xi}$, and χ_0^* is the curvature of the body at the point of separation .

By substituting the estimates (20) and (21) of the functions $d\ln v/d\eta$ and $d\beta/d\xi$ into the corresponding integrals in equation (19) and taking into account that

$$\lim_{\eta\to 0}\eta\int_0^\infty \frac{\eta'^2 d\eta'}{(\eta'^2-\eta^2)^2} = 0 \qquad \text{and} \qquad \lim_{\eta\to 0}\eta\int_0^\infty \frac{\xi'^2 d\eta'}{(\xi'^2+\eta^2)^2} = \frac{\pi}{4}\,,$$

we can find that the curvature of the free surface at the point of flow separation is equal to the curvature of the body, i.e.

$$\chi_0 = \lim_{\eta\to 0}\chi(\eta) = \chi_0^*\,. \quad (22)$$

NUMERICAL METHOD

The body shape is chosen to be a circular cylinder of radius R , the length of the closure interval being related to R as $S_{CD}/R = 10$. In discrete form, the solution is sought on a fixed set of points ξ_j , $j = 1,...,M$ distributed along the real axis of the parameter region and on a fixed set of points η_j , $j = 1,...,N$ distributed along its imaginary axis. The total number of points η_j was chosen in the range $N = 50-200$, and the total number of points ξ_j was chosen in the range $M = 3*N$ to check the convergence of the solution procedure. The points ξ_j are distributed so as to provide a higher density of the points $s_j = s(\xi_j)$ at points O and A , at which the derivative $ds/d\xi = \left|dz/d\varsigma\right|_{\varsigma=\xi}$ has singularities. The distribution of the points η_j is chosen so as to provide a higher density of the points $s_j = s(\eta_j)$ on the free surface near the point of flow separation.

The solution of equations (18) was found by the method of successive approximations applying the Hilbert transform to determine the (k + 1) -th approximation

$$\left(\frac{d(\ln v)}{d\eta}\right)^{(k+1)} = \frac{4}{\pi^2}\int_0^\infty F^{(k)}(\eta')\frac{\eta' d\eta'}{(\eta'^2-\eta^2)}\,, \qquad 0 < \eta < \eta_C\,, \quad (23)$$

$$F^{(k)}(\eta) = \frac{1}{1+\eta^2} + \frac{2}{\pi}\int_0^1 \left(\frac{d\beta}{d\xi'}\right)^{(k)}\frac{\xi' d\xi'}{\xi'^2+\eta^2} + \frac{WeK\eta}{2Rv^{(k)}}\left(1+\sigma-(v^{(k)})^2\right)\,, \quad (24)$$

where

$$v^{(k)}(\eta) = v_0 \exp\left(\int_0^{\eta} \left(\frac{d(\ln v)}{d\eta'} \right)^{(k)} d\eta' \right).$$

In each iteration step k the integro-differential equation (16) in the function $d\beta/d\xi$ was solved using the inner iteration procedure

$$\left(\frac{d\beta}{d\xi}\right)^{(l+1)} = \chi[s^{(l)}(\xi)] \frac{K^{(l)}\xi}{v_0} \left(\frac{1+\xi}{1-\xi}\right)^{\frac{1}{2}} \times$$
$$\exp\left[-\frac{1}{\pi} \int_0^1 \left(\frac{d\beta}{d\xi'}\right)^{(l)} \ln\left(\frac{\xi'-\xi}{\xi'+\xi}\right) d\xi' - \frac{1}{\pi} \int_0^{\infty} \left(\frac{d\ln v}{d\eta'}\right)^{(k)} \left(\pi - 2\tan^{-1}\left(\frac{\eta'}{\xi}\right)\right) d\eta' \right] \quad (2.26)$$

In each iteration step l the parameters $K^{(l)}$, η_C and S_w were calculated from equation (10), (13) and (15), respectively. The integrals appearing in the system of equations were evaluated using the linear interpolation of the functions $\beta(\xi)$ and $d(\ln v)/d\eta$ on the intervals (ξ_{j-1}, ξ_j) and (η_{j-1}, η_j), respectively. In the first iteration the functions $\beta(\xi)$ and $(d\ln v)/d\eta$ were given as $\beta(\xi) \equiv 0$ and $v(\eta) \equiv v_\infty$.

The convergence of the inner iteration procedure required 5 – 10 iterations to reach the condition $\left\| (d\beta/d\xi)^{l+1} - (d\beta/d\xi)^{l} \right\| < \varepsilon$. The convergence of the outer iterations required from several hundreds to several thousands of iterations, and it was obtained applying the under-relaxation method. The value of the relaxation parameter depends on the number N of nodes along the free surface. With increase in the number of nodes η_j, the relaxation parameter should be chosen smaller to provide the convergence of the solution. This is due to the singularity in the integral in (23), which is evaluated using the linear interpolation of the function $F(\eta)$ on the intervals $(\eta_{j-1/2}, \eta_{j+1/2})$.

REZULTS

Figure 2 shows the calculated results for cavity flow past a plate with a rounded edge of radius $R = 0.05H$. The cavity contour is depicted by a thin line, and the closing contour is depicted by a thick one. It can be seen that at large Weber numbers the flow parameters are little affected by surface tension. The effect of surface tension becomes noticeable at $We < 1000$, and in this case the cavity length and height decrease. It may be expected that with a further decrease in the Weber number the flow, in the limit, becomes free of cavitation.

Figure 3 shows the angle of flow turn on the rounded edge (the angle δ is shown in Figure 1) versus the Weber number for different values of the edge radius. At large Weber numbers when the effect of surface tension on the cavity flow parameters can be neglected, the flow turn angle depends on the edge radius as follows: the smaller the edge radius, the smaller the flow turn angle. In the limiting case of zero edge radius (a sharp edge), the flow turn angle tends to zero, which corresponds to the flow separating tangentially to the rectilinear part of the body. At Weber numbers smaller than 1000, the effect of surface tension becomes noticeable; the smaller the edge radius, the greater the Weber number at which this effect comes into play. It can be seen from Eq. (1) that the pressure drop across the cavity boundary in the neighborhood of the separation point increases with the edge curvature. Two characteristic regions can be distinguished in the graph: a region of strong dependence of the flow turn angle δ on the Weber number ($We < 200$) and a region of weak dependence ($We > 200$).

Figure 4 shows the angle of flow turn on the edge versus the Weber number at different cavitation numbers. With increasing cavitation number the flow turn angle decreases, i.e. the effect of the Weber number diminishes. For $We > 10^3$, the flow turn angle depends almost not at all on the Weber number or the cavitation number.

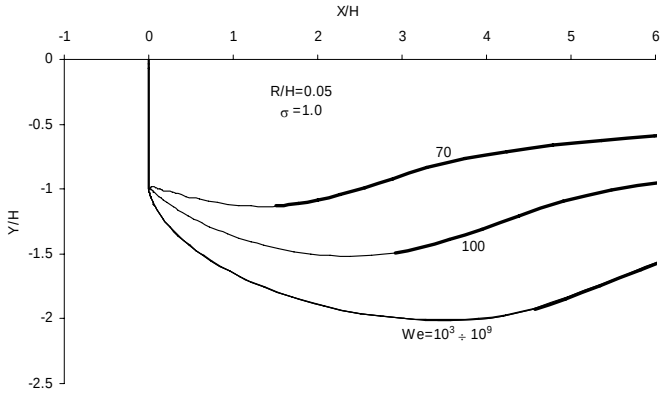

Figure 2: Effect of the Weber number on the cavity contour (thin lines) for cavity flow past a plate with edge radius $R = 0.05H$ at cavitation number $\sigma = 1.0$. The thick lines correspond to the cavity closure contours.

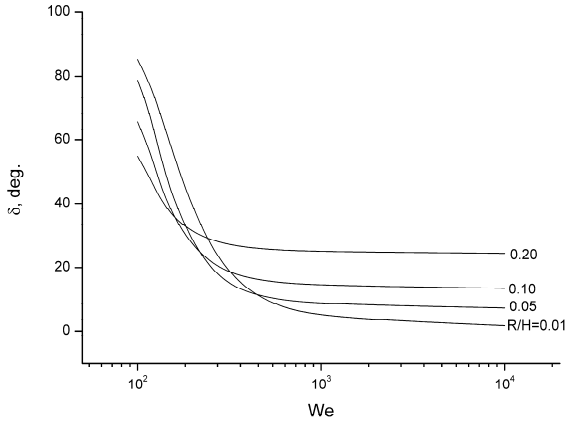

Figure 3: Angle of flow turn on the plate edge versus the Weber number for different edge radii at cavitation number $\sigma = 1.0$

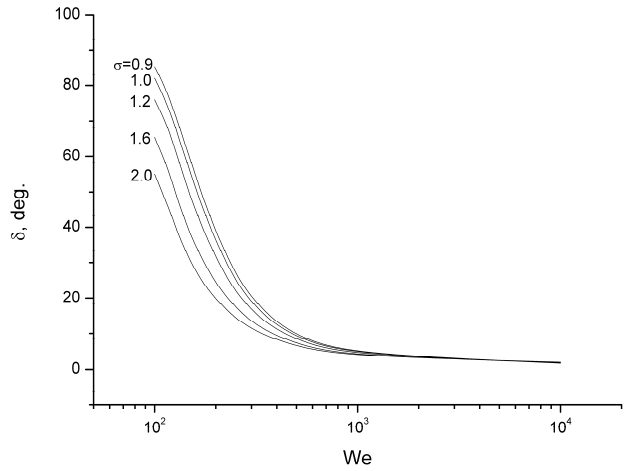

Figure 4: Effect of the cavitation number on the Weber number dependence of the flow turn angle for edge radius $R/H = 0.01$

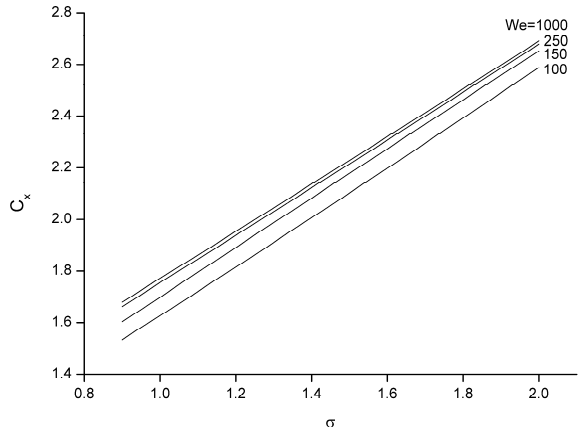

Figure 5: Effect of the cavitation number on the drag coefficient for edge radius $R/H = 0.01$

Figure 5 shows the drag coefficient versus the cavitation number for different Weber numbers at edge radius $R/H = 0.01$. The drag coefficient decreases somewhat as the Weber number decreases.

Figure 6 shows the effect of the Weber number in the range 200 to 2000 on the cavity flow parameters for entrance edge radius $R/H = 0.02$. Shown in the figure are the relative changes of the maximum cavity width, $\Delta h_c / h_c$, and the corresponding distance to the plate, $\Delta L_c / L_c$, as well as the relative change of the drag coefficient, $\Delta C_x / C_x$, versus the cavitation number. It can be seen that with decreasing cavitation number the effect of surface tension increases, and the change of the above flow parameters correlates with the change of the angle of flow turn on the entrance edge.

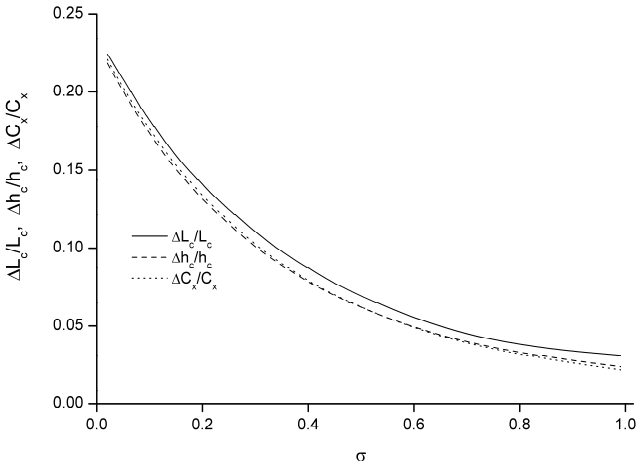

Figure 6: Relative change of the flow parameters at Weber numbers $We = 2000$ and $We = 200$ versus the cavitation number: the maximum cavity width $\Delta h_c / h_c$, the length $\Delta L_c / L_c$ corresponding thereto, and the drag coefficient $\Delta C_x / C_x$

Figure 6 shows the effect of the Weber number in the range 200 to 2000 on the cavity flow parameters for entrance edge radius $R/H = 0.02$. Shown in the figure are the relative changes of the maximum cavity width, $\Delta h_c / h_c$, and the corresponding distance to the plate, $\Delta L_c / L_c$, as well as the relative change of the drag coefficient, $\Delta C_x / C_x$, versus the cavitation number. It can be seen that with decreasing cavitation number the effect of surface tension increases, and the change of the above flow parameters correlates with the change of the angle of flow turn on the entrance edge.

CONCLUSION

The results presented above show that the effect of surface tension on the cavity flow parameters becomes noticeable at Weber numbers less that 10^3.

For supercavitating axisymmetric flows, a greater effect of surface tension on the flow parameters may be expected due to a greater curvature of the axisymmetric cavity, which has both a meridional and a radial component. Besides, the effect of surface tension increases with decreasing cavitator diameter, which appears in the Weber number as a characteristic dimension.

REFERENCES

[1] Vanden-Broeck, J.-M. (2004), "Nonlinear capillary free-surface flows". *J. of Engineering Mathematics*, 50, 415 – 426.

[2] Vanden-Broeck, J.-M. (1983) "The influence of surface tension on cavitating flow past a curved obstacles." *J. of Fluid Mech.* , 133, 255 – 264.

[3] Ackerberg, R.C. (1975) “The effects of capillarity on free-stream line separation.” *J. of Fluid Mech.*, 70, part 2, 333 – 352.
[4] Cumberbatch, E & Norbury, J. (1979) “Capillary modification of the singularity at a free-streamline separation point”, *Q.J. Mech. Appl. Maths.,* 32, 303 - 312.
[5] Joukovskii, N.E. (1890) “Modification of Kirchoff's method for determination of a fluid motion in two directions at a fixed velocity given on the unknown streamline, *Math. Coll.*, 15, 121 - 278.
[6] Chaplygin, S.A. (1910) “On the Pressure Exerted by a Plane-parallel Flow on Obstacles (on Airplane Theory)”. *Moscow: Moscow University*. 49 pp.
[7] Gurevich, M.I. (1965) Theory of Jets in Ideal Fluids. New York: Academic Press. 585 pp.
[8] Faltinsen, O.M. and Semenov, Y.A. (2008) “Nonlinear problem of flat-plate entry into an incompressible liquid”, *J. Fluid Mech.,* 611, 151 - 173.